



## The role of the NOP receptor in regulating food intake, meal pattern, and the excitability of proopiomelanocortin neurons

Borzoo Farhang<sup>a</sup>, Lindsay Pietruszewski<sup>a</sup>, Kabirullah Lutfy<sup>b</sup>, Edward J. Wagner<sup>a,\*</sup>

<sup>a</sup> College of Osteopathic Medicine, Western University of Health Sciences, Pomona, CA 91766, USA

<sup>b</sup> College of Pharmacy, Western University of Health Sciences, Pomona, CA 91766, USA

### ARTICLE INFO

#### Article history:

Received 30 September 2009

Received in revised form

17 May 2010

Accepted 18 May 2010

#### Keywords:

NOP receptor

OFQ

Nociceptin

Appetite

Glutamate

K<sup>+</sup> channels

### ABSTRACT

We evaluated the role of the nociceptin/orphanin FQ (NOP) receptor in regulating food intake, meal pattern and the activity of hypothalamic arcuate (ARC) neurons. The microstructural analysis of food intake and meal pattern was performed under both food-deprived and ad libitum conditions. Whole-cell patch clamp recordings were obtained using the *in vitro* hypothalamic slice preparation and biocytin-filled electrodes. NOP receptor knockout mice exhibited significantly reduced body weight. Fasting-induced hyperphagia was diminished for the first 2 h of a 6-h re-feeding period, and was associated with decreased meal duration and size, as well as a biphasic effect on meal frequency. The genotype effect observed under ad libitum conditions was comparatively unremarkable. Orphanin FQ/nociceptin (OFQ/N) was able to decrease evoked excitatory postsynaptic current amplitude, increase the S<sub>2</sub>:S<sub>1</sub> ratio via the paired-pulse paradigm, and decrease miniature excitatory postsynaptic current frequency in ARC neurons from wild type animals but not NOP receptor knockouts. In addition OFQ/N activated a reversible outward current that was antagonized by the G-protein activated, inwardly-rectifying K<sup>+</sup> (GIRK) channel blocker tertiapin in wild type but not NOP knockout animals. Both the presynaptic and postsynaptic actions of OFQ/N were observed in ARC neurons subsequently determined to be immunopositive for characteristic phenotypic markers of anorexigenic proopiomelanocortin (POMC) neurons. Taken together, these results demonstrate the contribution of the NOP receptor in controlling food intake and meal pattern, as well as glutamate release and GIRK1 channel activity at POMC synapses.

© 2010 Elsevier Ltd. All rights reserved.

### 1. Introduction

The nociceptin/orphanin FQ (NOP) receptor was discovered using homology screening in an attempt to clone as-of-then unknown subtypes of the opioid receptor family. Two groups nearly simultaneously uncovered a candidate with an amino acid sequence that predicted the serpentine arrangement of seven transmembrane-spanning domains, and a high degree of sequence homology to the  $\mu$ -,  $\kappa$ - and  $\delta$ -opioid receptor subtypes (Bunzow et al., 1994; Mollereau et al., 1994). Soon after, the endogenous ligand orphanin FQ (also known as nociceptin; OFQ/N) was discovered, and further characterization revealed it to be a hepta-decapeptide with consensus sequences found in other endogenous opioid peptides, most notably in dynorphin A<sub>1–17</sub>, which also has some affinity for the NOP receptor (Meunier et al., 1995; Reinscheid

et al., 1995; Zhang and Yu, 1995; Matthes et al., 1996). The NOP receptor associates with a pertussis-toxin sensitive, heterotrimeric G-protein (G<sub>i/o</sub>), and much like the other opioid receptor subtypes, subsequent ligand activation by OFQ/N results in reduced adenylyl cyclase activity and cAMP formation (Mollereau et al., 1994; Meunier et al., 1995; Reinscheid et al., 1995).

The NOP receptor exhibits a widespread distribution in the central nervous system, including, but not limited to, the cortex, spinal cord, amygdala and the hypothalamus (Bunzow et al., 1994). Within the hypothalamus, the NOP receptor is found in many different nuclei, including the ventromedial nucleus (VMN), paraventricular nucleus (PVN) and arcuate nucleus (ARC; Bunzow et al., 1994; Mollereau et al., 1994; Sinchak et al., 2006). The receptor localization exhibits considerable overlap with OFQ/N (Sinchak et al., 2006). The distribution of OFQ/N and NOP renders this system ideally suited to regulate homeostatic functions governed by the hypothalamus like reproduction and feeding. Indeed, OFQ/N stimulates sexual receptivity in estrogen-primed female rats (Sinchak et al., 2007). In addition, OFQ/N elicits a frank hyperphagia (Pomonis et al., 1996; Stratford et al., 1997; Polidori et al., 2000a; Economidou et al., 2006; Tajalli et al., 2006). OFQ/N also

\* Correspondence to: Edward J. Wagner, Ph.D., Department of Basic Medical Sciences, College of Osteopathic Medicine, Western University of Health Sciences, 309 E. Second Street, Pomona, CA 91766, USA.

E-mail address: [ewagner@westernu.edu](mailto:ewagner@westernu.edu) (E.J. Wagner).

decreases core body temperature (Chen et al., 2001; Blakley et al., 2004), suggesting that the neuropeptide may also regulate metabolism.

Cellularly, OFQ/N modulates neuronal excitability through both presynaptic and postsynaptic mechanisms. For example, it presynaptically inhibits glutamatergic and GABAergic synaptic currents in the periaqueductal gray (Vaughan et al., 1997), lateral amygdala (Meis and Pape, 2001) and suprachiasmatic nucleus (Gompf et al., 2005), and decreases aspartate and GABA release from cultured cortical neurons (Bianchi et al., 2004). OFQ/N also activates an inwardly-rectifying  $K^+$  conductance in oocytes co-expressing the mouse NOP receptor and the G-protein gated inwardly-rectifying  $K^+$  channel GIRK1 (Matthes et al., 1996), and in the dorsal raphe (Vaughan and Christie, 1996), locus coeruleus (Connor et al., 1996a), periaqueductal gray (Vaughan et al., 1997), ARC (Wagner et al., 1998), suprachiasmatic nucleus (Allen et al., 1999), VMN (Emmerson and Miller, 1999), nucleus raphe magnus (Pan et al., 2000) and in cultured tuberomammillary neurons (Bajic et al., 2004). In addition, OFQ/N inhibits calcium currents in SH-SY5Y cells (Connor et al., 1996b), in dissociated hippocampal neurons (Knoflach et al., 1996) and in rat sensory neurons (Abdulla and Smith, 1997), and it decreases calcium influx in neurons from the suprachiasmatic nucleus (Allen et al., 1999).

Thus, there is considerable evidence that OFQ/N inhibits neuronal activity throughout the peripheral and central nervous systems, including those areas involved in the control of appetite and energy intake. A neuroanatomical substrate of likely fundamental physiologic importance is the group of anorectic POMC neurons residing in the ARC. OFQ/N inhibits guinea pig ARC neurons, including those immunopositive for  $\beta$ -endorphin (Wagner et al., 1998), and it attenuates c-Fos expression in  $\alpha$ -melanocyte-stimulating hormone ( $\alpha$ -MSH) immunopositive neurons at meal termination (Bomberg et al., 2006). Moreover, both POMC-deficient and  $\beta$ -endorphin knockout mice exhibit hyperphagia and obesity (Appleyard et al., 2003; Challis et al., 2004). Thus, we tested the hypotheses that OFQ/N stimulates appetite in part through inhibition of POMC neurons by 1) presynaptically modulating glutamatergic input onto these neurons, and 2) postsynaptically modulating GIRK channels in these neurons, via activation of the NOP receptor.

## 2. Methods

### 2.1. Animals

All animal procedures described in this study are in accordance with institutional guidelines based on NIH standards. Animals were provided food and water *ad libitum*, maintained under constant temperature (25 °C) and kept on a 12-h light-dark cycle (ON – 07:00; OFF – 19:00). NOP receptor knockout mice (kindly provided by Dr. Hiroshi Takeshima, Tohoku Graduate School of Medicine, Japan) and their wild type littermate controls were obtained via the in-house mating of NOP heterozygous breeding pairs backcrossed for at least 8–12 generations on a C57BL/6 mouse strain. Genotyping of offspring was accomplished by isolating genomic DNA from a small piece of ear lobe obtained via ear punch while the animals were under isoflurane (2%) anesthesia. The following primers (SigmaGenosys, The Woodlands, TX, USA) were utilized: 1) a forward common primer (GCCATCGAGGTGTT CATGTGCCTGT), 2) a wild type primer (TGCCATACAAGACCTCCAGAAT) and 3) an NOP receptor knockout primer (CAATATCGCGGCTCAGTTCGAGGTGC). Amplicons used to identify wild type and mutant alleles were generated via PCR according the following protocol: 1) a 15-min incubation at 95 °C, 2) 30 cycles each consisting of a 30-s incubation at 94 °C, a 1-min incubation at 60 °C and a 1-min incubation at 72 °C, 3) a 5-min incubation at 72 °C and 4) a 2-min incubation at 4 °C.

### 2.2. Drugs

Unless otherwise indicated all drugs were purchased through Tocris Cookson, Inc. (Ellisville, MO, USA). OFQ/N, the voltage-gated  $Na^+$  channel blocker tetrodotoxin (TTX) with citrate (Alomone Labs, Jerusalem, Israel), the GIRK channel blocker tertipatin (Alomone), and the  $\gamma$ -aminobutyric acid (GABA)<sub>A</sub> receptor antagonist 6-imino-3-(4-methoxyphenyl)-1(6H)-pyridazinebutanoic acid hydrobromide (SR 95531) were dissolved in UltraPure H<sub>2</sub>O to stock concentrations of 1 mM, 1 mM,

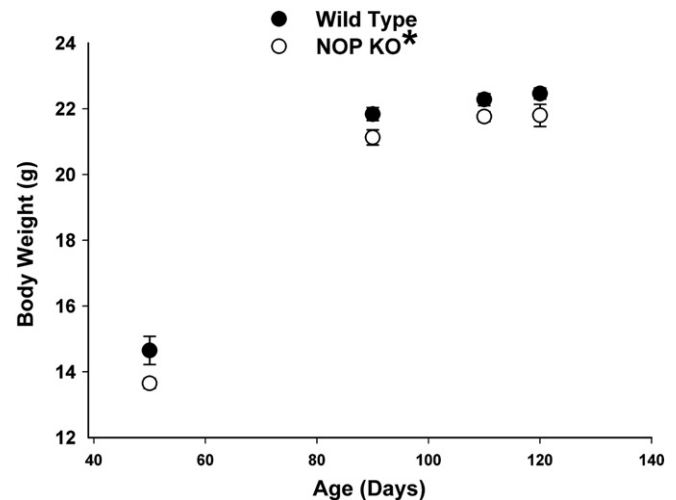


**Fig. 1.** Growth trajectories that illustrate the time-dependent weight gain in 50–120 day-old NOP receptor knockout animals and their wild type littermate controls. Symbols represent the means and vertical lines 2 S.E.M. of the body weight measured at 50, 90, 110, and 120 days of age. \*Body weight measured in NOP receptor knockout animals that is significantly different (repeated measures, multifactorial ANOVA/LSD;  $p < 0.05$ ;  $n = 8$ ) than that seen in their wild type littermates.

1  $\mu$ M, and 10 mM, respectively. The *N*-methyl-D-aspartate receptor antagonist *cis*-4-[Phosphomethyl]-2-piperidinecarboxylic acid (CGS 19755) was dissolved in 0.1 N NaOH and diluted to the appropriate volume with UltraPure H<sub>2</sub>O (final concentration 10 mM). The  $\alpha$ -amino-3-hydroxyl-5-methyl-4-isoxazole-propionate receptor antagonist 2,3-dioxo-6-nitro-1,2,3,4-tetrahydrobenzo[f]quinoxaline-7-sulfonamide (NBQX) was dissolved in DMSO to a stock concentration of 10 mM. Aliquots of these stock solutions were stored at –20 °C.

### 2.3. Feeding behavior

The microstructural analysis of feeding behavior in NOP receptor knockout mice and their wild type littermate controls (50–120 days old) was conducted as described previously (Ho et al., 2007; Diaz et al., 2009). A four-cage, Comprehensive Lab Animal Monitoring System (Columbus Instruments, Columbus, OH, USA) was used to monitor four parameters of feeding: food intake, meal duration, meal frequency and meal size. A meal was defined as an event in which an animal consumed  $\geq 10$  mg of food. Provided the animal had eaten at least this threshold amount, the instrumentation logged this event as a meal in the experimental data file the instant the animal withdrew its head from the food dish. The data file also contained information regarding the meal duration, which refers to the amount of time necessary to eat a meal. We also calculated the meal frequency as the number of meals consumed per unit time, and the meal size as the amount of food eaten in a given hour divided by the number of meals in that same hour. We validated our definition of a meal by executing a natural log transformation of the interbout (i.e., intermeal) interval and meal size data obtained from the fasting experiments in a manner similar to that previously described (Morgan et al., 2000; see [Supplementary material](#)). The data from both genotype conditions across the entire 6-h feeding window were combined together. The average interbout interval from all the data in these experiments was  $206.2 \pm 10.8$  s (range: 10–3566 s). Analysis of the frequency histogram and probability density of the transformed interbout interval revealed that the data closely approximated a unimodal distribution. Given the considerable variation in the meal frequency from the beginning to the end of the monitoring period (see Fig. 2), we also restricted our analysis to the first hour of the feeding window. Under these conditions the transformed interbout interval likewise exhibited a unimodal distribution that was very closely approximated by a normal, bell-shaped curve. The same held true when we evaluated the transformed meal size; regardless of whether we evaluated the data over the entire 6 h or just the first hour.

Feeding behavior was assessed with food and water freely available around the clock (*ad libitum* conditions) and, as mentioned above, under food-restricted conditions, in which the animals were fasted for 18 h prior to testing and given access to food for 6 h/day from 08:00 to 14:00. Water remains available *ad libitum*. The absolute intake of a powdered formulation of a standard mouse chow (Harlan Tekland Rodent Diet #8604) is taken as the total amount consumed at the end of either a 6- (for food-restricted) or 24-h (for *ad libitum*) monitoring session. The animals were allowed to acclimate in the feeding chambers for either 6 or 24 h per day over a three-day period. Each morning they were weighed and placed in their respective chambers for either 6 or 24 h. The food-restricted animals were returned

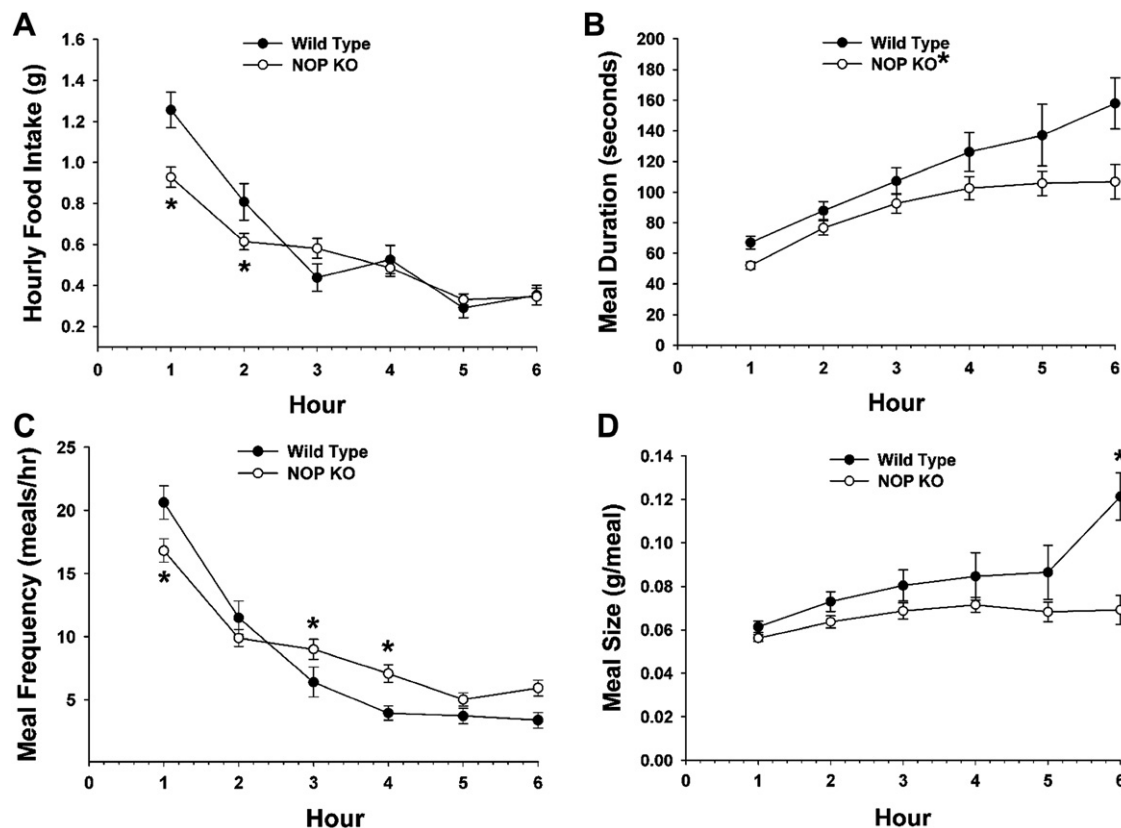


**Fig. 2.** Food intake and meal pattern as observed in fasted NOP knockout mice and their wild type littermate controls. Animals were weighed daily and introduced into their respective feeding cages and monitored over a 6-h window. (A) The hourly intake ingested at specific time points spanning the entire observation period. Symbols represent the mean and vertical lines 2 S.E.M. of the hourly food intake observed over the course of the 6 h window. (B) NOP-induced changes in meal duration. The symbols represent means and vertical lines 2 S.E.M. of the meal duration defined as the time necessary to ingest a meal  $\geq 10$  mg in mass. (C) NOP-induced changes in meal frequency. The symbols represent means and vertical lines 2 S.E.M. of the meal frequency defined as the number of meals ( $\geq 10$  mg) eaten per hour over the 6-h monitoring window. (D) NOP-induced changes in meal size. Symbols signify means and lines 2 S.E.M. of the amount of food consumed in a given hour divided by the number of meals in that same hour. \*Values taken from NOP knockout mice that are significantly different (repeated measures multifactorial ANOVA/LSD;  $p < 0.05$ ;  $n = 8$ ) than those from their wild type littermate controls.

to their home cages at the end of the 6 h, where they were fasted for the next 18 h. The ad libitum animals remained in their respective feeding chambers. After the three-day acclimation session, we initiated the seven-day monitoring phase during which the animals were weighed, immediately placed in their feeding chambers and then subjected to continuous monitoring of each of the four above-referenced feeding parameters over the 6- or 24-h time span. After completion of some of the feeding studies the animals were euthanized with isoflurane, the body length measured (naso-anal; in cm), and the subcutaneous fat dissected and weighed.

#### 2.4. Electrophysiology

On the day of experimentation, either an NOP receptor knockout or a wild type animal was lightly anesthetized with isoflurane, decapitated, its brain removed from the skull and the hypothalamus dissected between 09:00 and 10:00. We then mounted the resultant hypothalamic block on a cutting platform that was then secured in a vibratome well filled with an ice-cold, oxygenated (95%  $O_2$ , 5%  $CO_2$ ) artificial cerebrospinal fluid (aCSF) in which the considerable majority of sodium had been replaced by sucrose (sucrose, 208;  $NaHCO_3$ , 26; KCl, 2;  $NaH_2PO_4$ , 1.25; dextrose, 10; HEPES, 10;  $MgSO_4$ , 2;  $MgCl_2$  1;  $CaCl_2$ , 1; in mM.) Three to four coronal slices (300  $\mu$ m) through the rostro-caudal extent of the ARC, were cut at 1 °C. The slices were then transferred to an auxiliary chamber and incubated at room temperature in oxygenated aCSF containing (in mM): NaCl, 124;  $NaHCO_3$  26; dextrose, 10; HEPES, 10; KCl, 5;  $NaH_2PO_4$ , 2.6;  $MgSO_4$ , 2;  $CaCl_2$ , 1. They were kept under these conditions until electrophysiological recording.

During whole-cell patch recording from ARC neurons, slices were maintained in a chamber perfused with a warmed (35 °C), oxygenated aCSF in which the  $CaCl_2$  concentration was raised to 2 mM. Artificial CSF and all drugs (diluted with aCSF) were perfused via a peristaltic pump at a rate of 1.5 ml/min. Patch electrodes were assembled from borosilicate glass (World Precision Instruments; Sarasota, FL, USA; 1.5 mm O.D.) pulled on a P-97 Flaming Brown puller (Sutter Instrument Co., Novato, CA, USA), and filled with the following (in mM): potassium gluconate, 128; NaCl, 10;  $MgCl_2$ , 1; EGTA, 11; HEPES, 10; ATP, 1; GTP, 0.25; 0.5% biocytin; adjusted to a pH of 7.3 with KOH. For the studies designed to evaluate OFQ/N's ability to presynaptically

modulate amino acid neurotransmission, potassium gluconate was replaced with cesium gluconate. Electrode resistances varied from 3 to 8 M $\Omega$ . A Multiclamp 700A preamplifier (Axon Instruments, Foster City, CA, USA) amplified potentials and passed current through the electrode. Membrane currents were recorded in voltage clamp with access resistances that typically range from 8 to 22 M $\Omega$ , and underwent analog-digital conversion via a Digidata 1322A interface coupled to pClamp 8.2 software (Axon Instruments). The access resistance, as well as the resting membrane potential (RMP) and the input resistance ( $R_{in}$ ), were monitored throughout the course of the recording. If the access resistance deviated greater than 10% of its original value, the recording was ended. Low-pass filtering of the currents was conducted at a frequency of 2 KHz. The liquid junction potential was calculated to be  $-10$  mV, and corrected for during data analysis using pClamp software.

In the studies designed to evaluate evoked excitatory postsynaptic currents (eEPSCs) in arcuate neurons, concentric bipolar tungsten stimulating electrodes (World Precision Instruments) were placed 0.5–1.0 mm lateral to the recording electrode to deliver square-wave pulses 500  $\mu$ s in duration (0.1 Hz; 3–18 V) generated by a model S88 K stimulator (Astro-Med, Inc., West Warwick, RI, USA) and converted to constant voltage by a model SIU5 stimulus isolation unit (Astro-Med). We recorded eEPSCs from a holding potential of  $-75$  mV in the presence of SR 95531 (10  $\mu$ M) to block  $GABA_A$  receptor-mediated synaptic currents. We employed the paired-pulse paradigm in which we presented successive stimuli that were separated by 75 ms from one another. Peak eEPSC amplitudes were measured by averaging those obtained from 20 consecutive stimulations. Rare failures of the stimulus to evoke EPSCs were excluded from the analyses. Cells were perfused with OFQ/N (100 nM–1  $\mu$ M) for 4 min and the stimulation paradigm are repeated in the presence of the peptide.

We recorded miniature EPSCs (mEPSCs) in the presence of both SR 95531 (10  $\mu$ M) and TTX (500 nM) from a holding potential of  $-75$  mV. After collecting a 3–4 min segment of baseline data, we perfused OFQ/N (1  $\mu$ M) for 4 min, and then recorded mEPSCs in the presence of the peptide. The threshold for mEPSC detection was set at least 3 pA below the baseline holding current as assessed from the headstage output, and continuously monitored throughout each 3–4 min recording period. Information on interval and amplitude was obtained from at least 100

contiguous mEPSCs, which we used to evaluate OFQ-induced alterations in mEPSC frequency and amplitude as assessed from cumulative probabilities generated via a quantile plot of the raw data.

To characterize the OFQ/N-induced activation of GIRK, the peptide was perfused until a new steady-state holding current was established (3–5 min). Current–voltage relationships were generated before and immediately following agonist application over a range centering on the equilibrium potential for  $K^+$ . This is accomplished with step command potentials ranging from  $-50$  to  $-130$  mV (1 s duration; 10 mV increments). The ability of OFQ/N (1  $\mu$ M) to elicit an outward current was ascertained prior to, and in the presence of, the GIRK channel blocker tertiapin (10 nM).

### 2.5. Immunohistochemistry

Following electrophysiological recording, slices were fixed with 4% paraformaldehyde (PFM) in Sorensen's phosphate buffer (pH 7.4) for 90–180 min (Ronnekleiv et al., 1990). They then were immersed overnight in 20% sucrose dissolved in Sorensen's buffer, and frozen in Tissue-Tek embedding medium (Miles, Inc., Elkhart, IN, USA) the next day. Coronal sections (16  $\mu$ m) were cut on a cryostat, and mounted on slides. These sections were washed with 0.1 M sodium phosphate buffer (pH 7.4), and then processed with streptavidin-Alexa Fluor (AF)488 (Molecular Probes, Inc., Eugene, OR, USA) at a 1:300 dilution. After localizing the biocytin-filled neuron via fluorescence microscopy, the slides containing the appropriate sections were processed with polyclonal antibodies directed against either the NOP receptor (Santa Cruz Biotechnology, Inc., Santa Cruz, CA, USA; 1:500 dilution), the  $K_{IR}3.1$  (GIRK1) channel (Alomone; 1:200 dilution), cocaine-amphetamine regulated transcript (CART; Phoenix Pharmaceuticals, Inc., Belmont, CA, USA; 1:2000 dilution) or  $\alpha$ -MSH (Immunostar, Inc., Hudson, WI, USA; 1:200 dilution) using fluorescence immunohistochemistry (Ronnekleiv et al., 1990).

### 2.6. Statistics

Comparisons between two groups were made using the Student's *t*-test. Comparisons between more than two groups were performed using a repeated measures, multifactorial analysis of variance (ANOVA), followed by the Least Significant Difference (LSD) test. If we encountered a significant interaction then we performed a one-way ANOVA followed by the LSD test to assess potential genotype differences at a given time point. Differences were considered statistically significant if the probability of error was less than 5%.

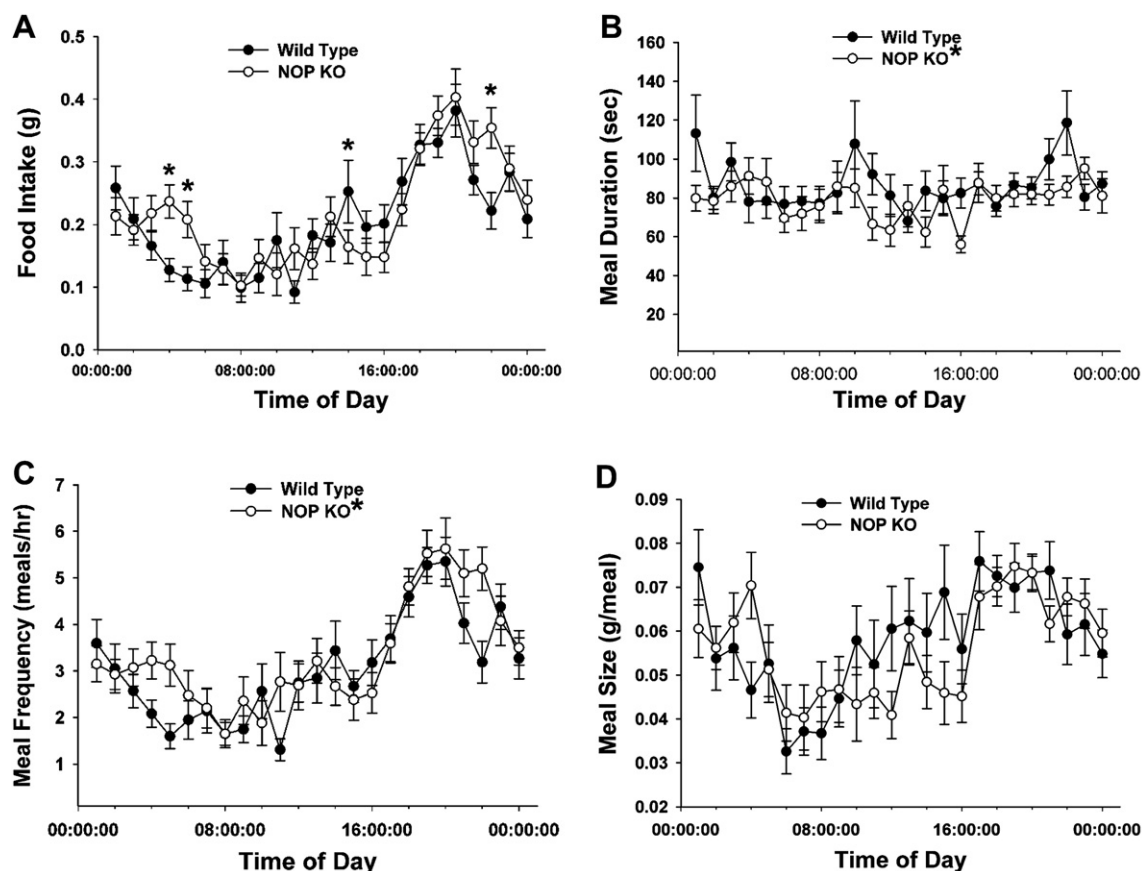
## 3. Results

Fig. 1 shows the body weights of NOP receptor knockouts and their wild type littermate controls (50–120 days of age) measured at different time points over the study period. A repeated measures, multifactorial ANOVA indicated significant main effects of genotype ( $F(1,3) = 7.75$ ,  $p < 0.01$ ) and time ( $F(1,5) = 378.60$ ,  $p < 0.0001$ ), with no significant interaction between the two variables ( $F(1,1) = 0.25$ ,  $p < 0.87$ ). Thus, NOP receptor knockouts displayed a comparatively lower body weight at each of the time points evaluated. Subcutaneous fat deposition and body lengths measured in these animals were 62% and 97%, respectively, of the average values encountered in the wild type controls ( $0.31 \pm 0.04$  g vs.  $0.49 \pm 0.09$  g;  $p < 0.13$ ;  $8.2 \pm 0.1$  cm vs.  $8.5 \pm 0.2$  cm;  $p < 0.33$ ;  $n = 4-5$ ). In order to more fully assess the role of the NOP receptor in regulating energy homeostasis, we initially examined feeding behavior over a 6-h window for seven days in food-deprived NOP knockout mice and their wild type littermate controls that were fasted for 18 h prior to experimentation. Fig. 2A depicts food intake as a function of time over the course of the 6-h monitoring period. A repeated measures, multifactorial ANOVA revealed a robust main effect of time ( $F(1,5) = 49.65$ ,  $p < 0.0001$ ), a nearly significant main effect of genotype ( $F(1,5) = 3.73$ ,  $p < 0.06$ ), and a highly significant interaction between the variables ( $F(1,1) = 4.31$ ,  $p < 0.001$ ). Subsequent post-hoc multiple range analysis demonstrated that NOP knockout mice exhibit a significantly reduced food intake at 1 and 2 h into the monitoring period as compared to wild type littermate controls. A very similar pattern emerged when intake was normalized to the animal's body weight (time ( $F(1,5) = 74.34$ ,  $p < 0.0001$ ); genotype ( $F(1,5) = 8.62$ ,  $p < 0.004$ ); interaction ( $F(1,1) = 3.87$ ,  $p < 0.03$ ; not shown)). We also examined the impact of the NOP receptor on meal duration, frequency and size. Fig. 2B shows the meal duration

ascertained every hour during the evaluation period. There were significant main effects of genotype ( $F(1,5) = 22.80$ ,  $p < 0.0001$ ) and time ( $F(1,5) = 20.70$ ,  $p < 0.0001$ ), with no interaction between the two variables ( $F(1,1) = 1.24$ ,  $p < 0.29$ ); indicating that the meals ingested by the NOP receptor knockout mice were of shorter duration throughout the monitoring period. Evaluation of meal frequency showed a significant main effect of time ( $F(1,5) = 71.30$ ,  $p < 0.0001$ ) but not of genotype ( $F(1,5) = 1.55$ ,  $p < 0.22$ ). There was, however, a highly significant interaction between the two variables ( $F(1,1) = 4.54$ ,  $p < 0.001$ ). Post-hoc testing suggested a biphasic pattern for meal frequency – with NOP receptor knockout mice consuming meals at a reduced frequency during the first hour, and at an increased frequency during the third and fourth hours of the daily observation period (Fig. 2C). The decreases in food intake and meal duration, coupled with the latent increase in meal frequency, effectively translated into a reduced meal size in these animals (time ( $F(1,5) = 7.92$ ,  $p < 0.0001$ ); genotype ( $F(1,5) = 27.55$ ,  $p < 0.0001$ ); interaction ( $F(1,1) = 3.47$ ,  $p < 0.005$ ; Fig. 2D)).

Some of these differences in meal pattern and body weight persisted under ad libitum conditions (Fig. 3). For example, analysis of hourly intake evaluated around the clock revealed significant main effects of genotype ( $F(1,23) = 15.41$ ,  $p < 0.001$ ) and time ( $F(1,23) = 16.74$ ,  $p < 0.0001$ ), as well as a significant interaction ( $F(1,1) = 1.72$ ,  $p < 0.02$ ). Subsequent post-hoc analysis indicated that NOP receptor knockout animals exhibit increased nocturnal feeding at 22:00, 04:00 and 05:00 h, and decreased intake in the afternoon at 14:00 h (Fig. 3A). This significant effect of genotype, however, was not substantiated when looking at cumulative 24-h intake (not shown). Ad libitum meal duration was nearly identical to that observed under food-deprived conditions – namely, there were significant main effects of genotype ( $F(1,23) = 7.89$ ,  $p < 0.01$ ) and time ( $F(1,23) = 1.69$ ,  $p < 0.03$ ), with no significant interaction between the two variables ( $F(1,1) = 1.18$ ,  $p < 0.25$ ; Fig. 3B). As shown in Fig. 3C we also found significant main effects of genotype ( $F(1,23) = 4.73$ ,  $p < 0.03$ ) and time ( $F(1,23) = 11.10$ ,  $p < 0.0001$ ) on ad libitum meal frequency, with no significant interaction between the two variables ( $F(1,1) = 1.28$ ,  $p < 0.17$ ). Thus, NOP receptor knockout animals exhibit increased meal frequency under these conditions, which is similar to latent increase seen under food-restricted conditions. With regard to ad libitum meal size we detected a significant main effect of time ( $F(1,23) = 4.80$ ,  $p < 0.0001$ ) but not of genotype ( $F(1,23) = 1.08$ ,  $p < 0.30$ ), and no significant interaction between the two variables ( $F(1,1) = 1.25$ ,  $p < 0.20$ ). This contrasts with what we observed under fasting conditions.

We next sought to determine the role of the NOP receptor in modulating the activity of neurons involved in the control of the hypothalamic feeding circuitry. Initially, we examined the effects of OFQ/N on eEPSC amplitude and the  $S_2:S_1$  ratio using the paired-pulse paradigm. As illustrated by the traces of an ARC neuron from a wild type mouse shown in Fig. 4, OFQ/N produced a reversible and dose-dependent decrease in the amplitude of the EPSC evoked by the  $S_1$  stimulus, concomitant with an increase in the  $S_2:S_1$  ratio, which is indicative of a presynaptic effect of the peptide. To further verify a presynaptic inhibition of glutamate release at synapses of ARC neurons, we next evaluated the effects of OFQ/N on mEPSC frequency. From the membrane current traces in Fig. 5A and the cumulative probability plot in Fig. 5B, it is apparent that OFQ/N increased the interval between contiguous mEPSCs. Since mEPSC interval is the inverse of mEPSC frequency, this corresponds to a decrease in mEPSC frequency. Indeed, OFQ/N reduced mEPSC frequency to 42% of baseline, with no discernable effect on mEPSC amplitude (Fig. 5C). These mEPSCs were sensitive to antagonism to ionotropic glutamate receptor blockers (not shown). However, in a recording of a neuron from an NOP knockout animal, this effect



**Fig. 3.** NOP-induced changes in hourly food intake (A), meal duration (B), meal frequency (C) and meal size under ad libitum conditions. (A) The symbols represent means and vertical lines 2 S.E.M. of the hourly amount of food consumed over a 24-h period. (B) Symbols represent the mean and vertical lines 2 S.E.M. of the meal duration measured over a 24-h period. (C) Symbols represent the mean and vertical lines 2 S.E.M. of the meal frequency measured over a 24-h period. (D) Symbols represent the mean and vertical lines 2 S.E.M. of the meal size measured over a 24-h period. \*Values taken from NOP knockout mice that are significantly different (repeated measures multifactorial ANOVA/LSD;  $p < 0.05$ ;  $n = 8$ ) than those from their wild type littermate controls.

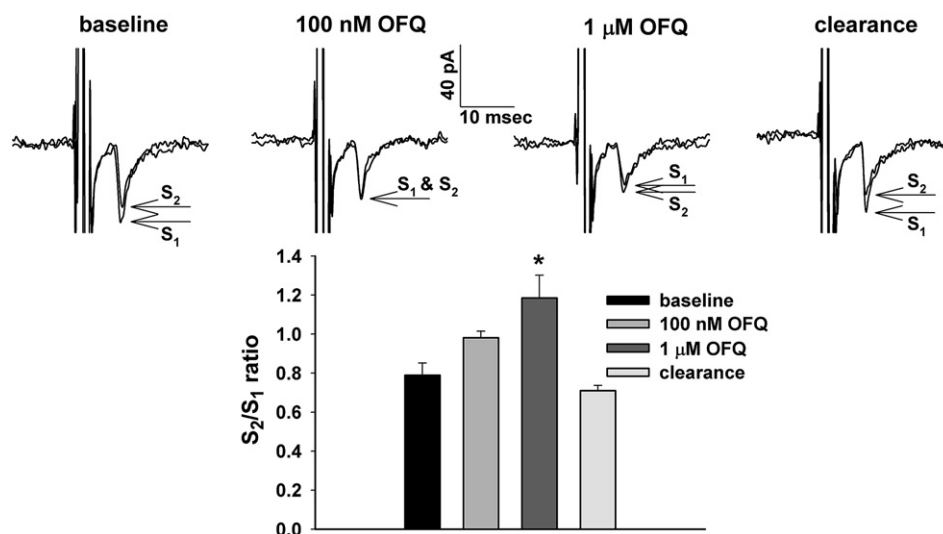


**Fig. 4.** OFQ/N decreases eEPSC amplitude and increases the  $S_2:S_1$  ratio in ARC neurons. **Top** – traces of membrane current obtained during a recording of an ARC neuron from a wild type animal that represent eEPSCs triggered via the paired-pulse paradigm (from left) at baseline, in the presence of 100 nM and 1  $\mu$ M OFQ/N, and following clearance of the neuropeptide from the slice. Note the reversible decrease in the amplitude of the eEPSC elicited by the  $S_1$  stimulus. **Bottom** – a bar graph that illustrates the reversible dose-dependent increase in the  $S_2:S_1$  ratio. Bars represent means and vertical lines 1 S.E.M. of the  $S_2:S_1$  ratio. \*Values from OFQ/N-treated slices that were significantly different (one-way ANOVA/LSD;  $p < 0.05$ ;  $n = 4$ ) from baseline control.



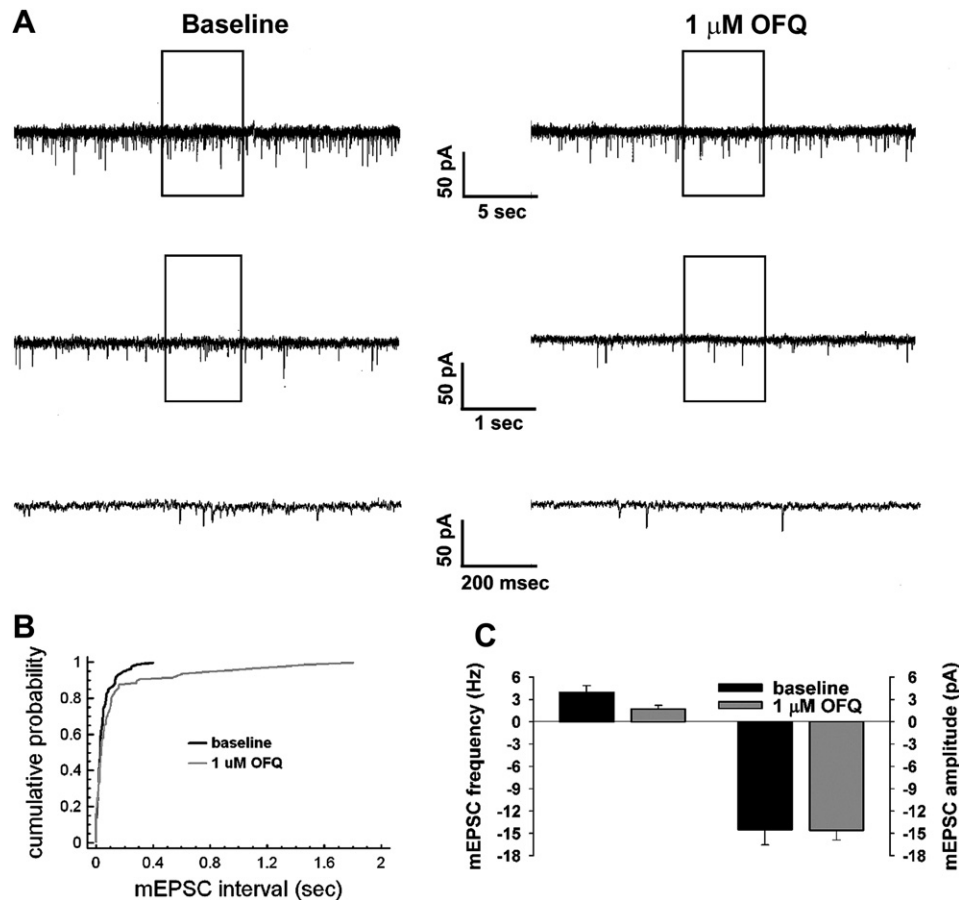


**Fig. 5.** OFQ/N selectively decreases mEPSC frequency in ARC neurons. **A**, Membrane current traces showing the spontaneous mEPSCs recorded in an ARC neuron from a wild type control animal at a holding potential of  $-75$  mV in the presence of  $10$   $\mu$ M SR 95531 and  $500$  nM TTX. The middle traces represent excerpts from expanded portions of their respective upper traces that are contained within the bracket. The lower traces, in turn, represent excerpts from expanded portions of their respective middle traces that are contained within the bracket. The frequency of the robust mEPSCs occurring under baseline control conditions (left) is reduced by  $1$   $\mu$ M OFQ/N (right). **B**, Cumulative probability plot that illustrates the increase in the interval, which is the inverse of frequency, between contiguous mEPSCs observed in the cell in **A**. **C**, Composite bar graph illustrating that OFQ/N decreases mEPSC frequency over  $50\%$  (from  $4.0 \pm 0.9$  Hz to  $1.7 \pm 0.5$  Hz;  $n = 8$ ) without affecting mEPSC amplitude. Bars represent means and vertical lines  $1$  S.E.M. of the mEPSC frequency (left) and amplitude (right) measured in ARC neurons obtained under baseline conditions (black columns) and in the presence of  $1$   $\mu$ M OFQ/N (gray columns).

was negated. The robust mEPSCs shown in Fig. 6A were impervious to bath application of OFQ/N, with the mEPSC interval (Fig. 6A and B), frequency and amplitude (Fig. 6C) virtually identical to those observed under baseline control conditions. Despite this lack of response to OFQ/N, the mEPSCs were largely abolished by bath application of ionotropic glutamate receptor antagonists (Fig. 6A). Both of the wild type ARC neurons shown in Figs. 4 and 5 were determined to be immunopositive for the NOP receptor, whereas the neuron from the NOP receptor knockout animal shown in Fig. 6 was not (Fig. 7). Collectively, this suggests that OFQ/N can act presynaptically via an NOP receptor-mediated mechanism to decrease the release of glutamate from nerve terminals impinging upon ARC neurons.

We also examined the potential of the NOP receptor to activate postsynaptic GIRK channels in ARC neurons using NOP receptor knockout mice and their wild type controls. The membrane current trace shown in Fig. 8A was produced in a recording of an ARC neuron from a wild type control animal. OFQ/N induced a modest outward current that was reversible upon clearance of the neuropeptide from the slice (Fig. 8A;  $n = 10$ ). An examination of the I/V plot shown in Fig. 8B and derived from I/V relationships generated prior to, and in the presence of, OFQ/N revealed several important features of this putative postsynaptic response. Firstly, the OFQ/N-induced outward current reversed polarity near the Nernst equilibrium potential for  $K^+$ . Secondly, OFQ/N increased cell conductance as estimated from

linear portions of the slope of the I/V plot via linear regression. Moreover, the inward current and cell conductance observed at potentials hyperpolarized with respect to the reversal potential increased markedly, and this is further substantiated in Fig. 8C. The OFQ/N-induced outward current and increase in conductance were considerably attenuated in the presence of the GIRK channel blocker tertiapin ( $10$  nM; Fig. 9A and B;  $n = 3$ ), associated with immunoreactivity for the GIRK1 channel (Fig. 9C), and altogether absent in recordings of ARC neurons from NOP knockout animals (Fig. 9D;  $\Delta g_{-60 \text{ to } -80 \text{ mV}}: 0.04 \pm 0.09$  nS;  $\Delta g_{-100 \text{ to } -130 \text{ mV}}: -0.09 \pm 0.11$  nS;  $n = 4$ ). All of these effects were observed in ARC neurons that were immunopositive for anorexigenic CART ( $n = 5$ ; Fig. 10), which has long been known to colocalize in POMC neurons (Lambert et al., 1998; Horvath, 2005), as well as  $\alpha$ -MSH ( $n = 3$ ; not shown). Taken together, this suggests that OFQ/N also can directly inhibit ARC neurons, including POMC neurons, via both a presynaptic inhibition of glutamatergic input, and a positive modulation of a GIRK1 channel upon activation of NOP receptors.

#### 4. Discussion

The results of the present study reveal the role of the NOP receptor in regulating food intake and meal pattern that involves presynaptic and postsynaptic inhibition of ARC POMC neuronal activity. This conclusion is based on the following observations: 1)

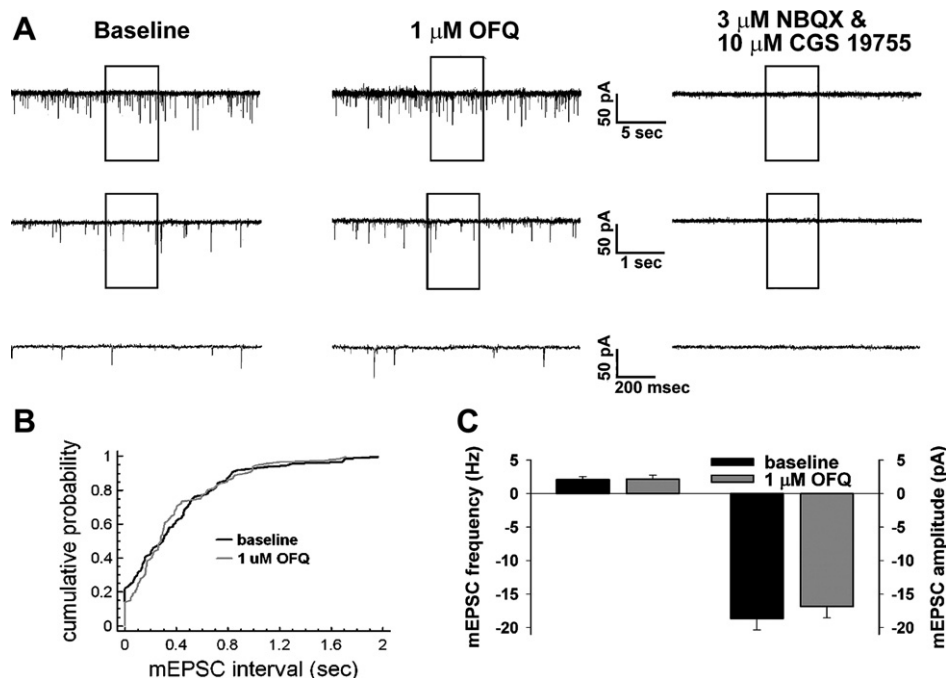


**Fig. 6.** Lack of effect of OFQ/N on mEPSC frequency in ARC neurons from NOP knockout animals. **A**, Membrane current traces showing the spontaneous mEPSCs recorded in an ARC neuron from an NOP receptor knockout animal. The frequency of the robust mEPSCs occurring under baseline control conditions (left) is unaltered by 1  $\mu\text{M}$  OFQ/N (middle), but they are markedly attenuated in the presence of 3  $\mu\text{M}$  NBQX and 10  $\mu\text{M}$  CGS 19755 (right). **B**, Cumulative probability plot that illustrates the lack of effect of OFQ/N on the interval, which is the inverse of frequency, between contiguous mEPSCs observed in the cell in **A**. **C**, Composite bar graph illustrating that OFQ/N was without effect on both mEPSC frequency and mEPSC amplitude. Bars represent means and vertical lines 1 S.E.M. of the mEPSC frequency (left) and amplitude (right) obtained under baseline conditions (black columns;  $n = 5$ ) and in the presence of 1  $\mu\text{M}$  OFQ/N (gray columns;  $n = 5$ ).

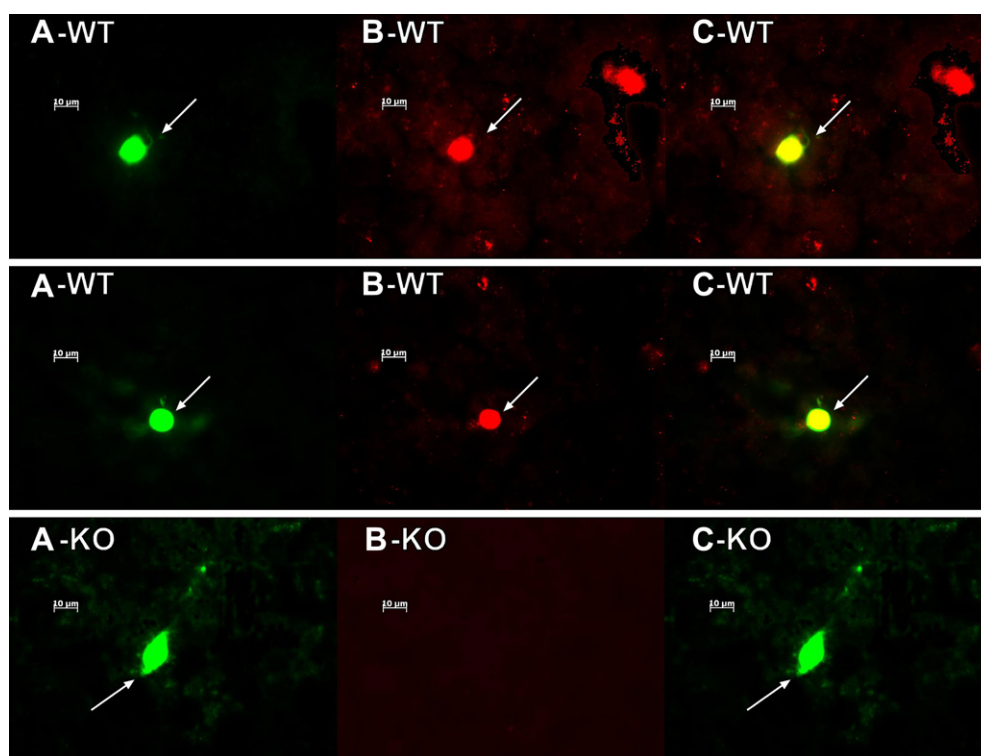


**Fig. 7.** ARC neurons from wild type animals express the NOP receptor, whereas those from NOP receptor knockout animals do not. The **top** and **middle** rows depict neurons from wild type animals whose recordings are shown in Figs. 4 and 5, respectively, whereas the **bottom** row represents a neuron from an NOP knockout animal whose recording is shown in Fig. 6. The left column (**A**) shows the biocytin labeling with streptavidin-AF488. The middle column (**B**) shows the NOP immunoreactivity as visualized with AF546. The right column (**C**) represents the composite overlay of the double labeling. All color photomicrographs were taken at 40 $\times$  magnification.

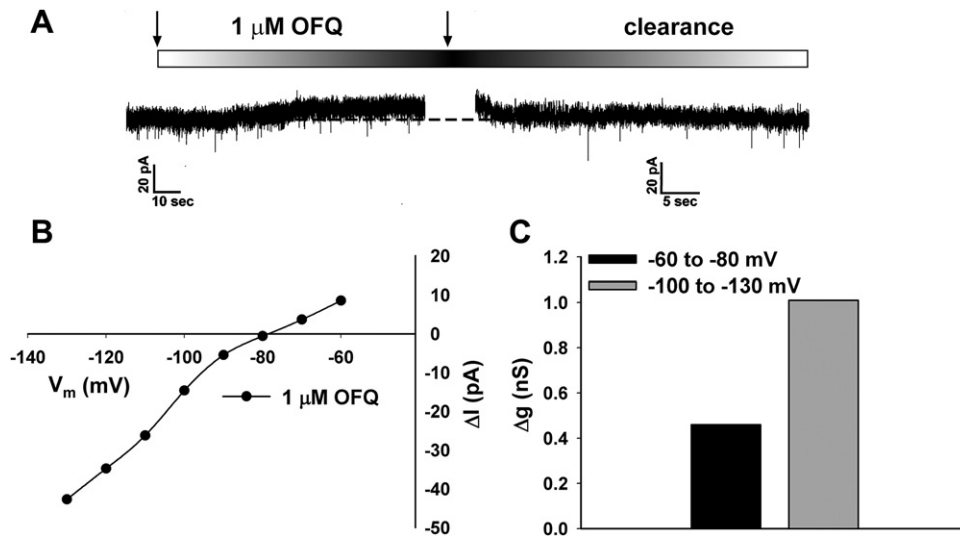


**Fig. 8.** **A**, A reversible outward current elicited by OFQ/N in an ARC neuron from a wild type control animal. This outward current was produced by OFQ/N (1  $\mu$ M) from a holding potential of  $-60$  mV in the presence of 500 nM TTX. The break in the trace in the upper panel represents the time necessary to conduct a second I/V relationship, and the early stages of OFQ/N clearance from the slice. **B**, An I/V plot that reveals the OFQ/N-induced increase in slope conductance as well as the reversal potential ( $-78$  mV) near the Nernst equilibrium potential for  $K^+$ . The symbols represent the changes in membrane current ( $\Delta I$ ) observed at different membrane voltages ( $V_m$ ) that were caused by OFQ/N. **C**, A bar graph that illustrates the increase in slope conductance estimated by linear regression between  $-60$  &  $-80$  mV was 0.46 nS, whereas that between  $-100$  &  $-130$  mV was more pronounced (1.01 nS; rectification ratio: 2.2).

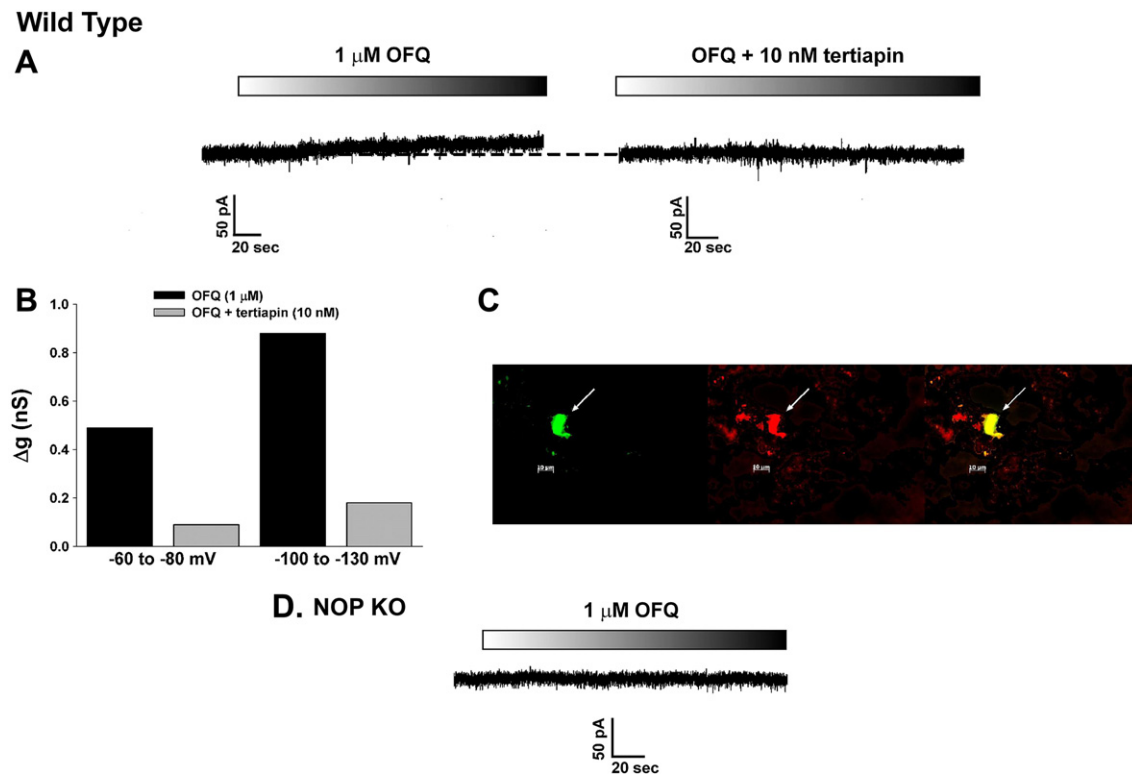


**Fig. 9.** The OFQ/N-induced outward current observed in wild type ARC neurons is markedly attenuated by the GIRK channel blocker tertipatin. **A**, The membrane current trace on the left shows the outward current elicited by 1  $\mu$ M OFQ/N, which was largely abolished in the presence of tertipatin (10 nM) as evidenced from the trace on the right. **B**, A bar graph that illustrates the sizable diminution in the OFQ/N-induced change in slope conductance ( $\Delta g$ ) estimated by linear regression between  $-60$  and  $-80$  mV, and between  $-100$  and  $-130$  mV, caused by tertipatin. Bars represent the  $\Delta g$  measured in the cell in **A** between  $-60$  and  $-80$  mV, and between  $-100$  and  $-130$  mV, in the presence of either OFQ/N alone or the combination of tertipatin and OFQ/N. **C**, Color photomicrographs showing the localization of GIRK1 channel immunoreactivity in the cell in **A**. The photomicrograph on the left shows the biocytin labeling with streptavidin-AF488. The photomicrograph in the middle shows the GIRK1 channel immunoreactivity as visualized by AF546. The photomicrograph on the right shows the composite overlay. All photomicrographs were shot at 63 $\times$  magnification. **D**, This trace shows the lack of an OFQ/N-induced activation of GIRK channels in an ARC neuron from a NOP receptor knockout animal.



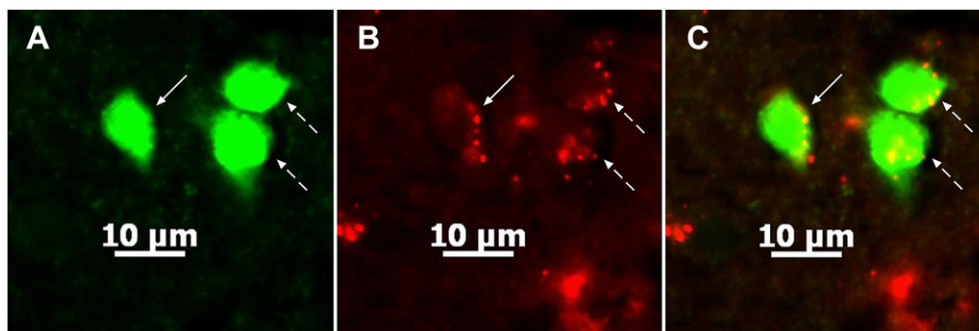


**Fig. 10.** Double labeling of an ARC neuron (denoted by solid arrow) that is electrotonically coupled to two other cells (denoted by the dashed arrows) and immunopositive for phenotypic markers characteristic of POMC neurons. The recorded cell (denoted by solid arrow) responded to 1  $\mu$ M OFQ/N with a 53% reduction in mEPSC frequency. **A**, A color photomicrograph that illustrates the biocytin labeling as visualized with streptavidin-AF488. **B**, A color photomicrograph illustrating the punctate CART immunostaining seen in the cells in **A** as visualized with AF546. **C**, A composite overlay illustrating the double labeling of these ARC neurons.

NOP receptor knockout mice exhibited reduced food intake under fasted conditions, which corresponded with a reduced average daily body weight, 2) they also displayed reduced meal duration frequency and size under these conditions, and 3) the OFQ/N-induced presynaptic inhibition of glutamatergic input onto ARC POMC neurons observed in wild type controls was absent in NOP receptor knockout mice, as was the postsynaptic activation of the GIRK1 channel.

From the microstructural analysis performed in the present study, it is evident that the NOP receptor plays a more important role in stimulating food intake under food-deprived conditions. The fasting-induced hyperphagia was blunted in NOP receptor knockout animals. It was most marked in the early stages of the feeding session, with significant diminution observed upto 2 h that eventually resolved by the end of the monitoring, and may be due to an inability of the OFQ/N peptide to bind its cognate NOP receptor and thereby inhibit the excitability of anorexigenic POMC neurons. This finding is similar to those described in a recent report by Koizumi et al. (2009), in which they showed that NOP receptor knockout animals exhibited a lower preference for a high sucrose diet and a reduced intake of a high fat diet under food-deprived but not ad libitum conditions. On the other hand, reduction in the level of NOP receptor expression caused by antisense oligonucleotides leads to decreases in both circulating corticosterone levels and time spent in the open arms of the elevated plus maze (Blakley et al., 2004). This suggests that the NOP receptor null mice are more anxious and less able to cope appropriately to the stress of food-deprivation.

The present study also provides the very first microstructural analysis demonstrating how the NOP receptor regulates meal pattern. It has been reported that OFQ/N suppresses CART gene expression (Bungo et al., 2009), and c-Fos expression in POMC neurons in response to satiation (Bomberg et al., 2006). This suggests an important role for the NOP receptor in regulating the consummatory aspects of feeding behavior, and is in keeping with our present findings that NOP receptor knockout animals exhibit a reduced intake during the first 2 h of the monitoring period, as well as decreased meal duration and size. These animals also exhibit a diminished meal frequency during the first hour of food-restricted feeding. This is supportive of an additional role for the NOP receptor in regulating the appetitive component of feeding, and is in agreement with the fact that OFQ/N increases the expression of orexigenic agouti-related peptide (AgRP; Bungo et al., 2009). The fact that these changes in meal pattern at least partially transcend specific intake conditions demonstrates the physiological relevance of the NOP receptor in regulating meal pattern. Also transcending specific intake conditions was the decreased growth trajectory of the NOP receptor knockout animals. However, their

food intake was not significantly reduced under ad libitum conditions. Given the ability of OFQ/N to lower core body temperature and reduce uncoupling protein 1 expression in brown adipose tissue (Chen et al., 2001; Blakley et al., 2004; Matsushita et al., 2009), as well as the increased resting core body temperature (Uezu et al., 2004), it follows that the reduced average daily weight seen in these animals can be attributed to an increased energy expenditure in these animals. This will be confirmed in future experiments designed to evaluate the respiratory exchange ratio and metabolic heat production in NOP receptor knockout mice and their wild type littermate controls.

Our findings also show that OFQ/N presynaptically inhibits glutamatergic neurotransmission at POMC synapses in wild type but not NOP receptor knockout animals. This is consistent with what has been observed in ARC neurons from immature rats (Emmerson and Miller, 1999), as well as in the periaqueductal gray (Vaughan et al., 1997), amygdala (Meis and Pape, 2001) and the hypothalamic suprachiasmatic nucleus (Gompf et al., 2005). Glutamate is the predominant excitatory neurotransmitter in the hypothalamus (van den Pol et al., 1990; Brann and Mahesh, 1995), and provides a fundamentally important depolarizing signal that helps drive hypothalamic cells towards threshold for firing  $\text{Na}^+$ -dependent action potentials. The NOP receptor-mediated presynaptic inhibition of glutamate release at POMC synapses would therefore reduce excitatory tone onto these cells. In addition, we observed that OFQ/N activated a postsynaptic GIRK1 channel in wild type but not NOP receptor knockout animals. This is in agreement with what has been shown previously in immature rat (Emmerson and Miller, 1999) and guinea pig ARC neurons (Wagner et al., 1998), in the VMN (Emmerson and Miller, 1999) and supra-chiasmatic (Allen et al., 1999) nucleus, as well as the in dorsal raphe (Vaughan and Christie, 1996), locus coeruleus (Connor et al., 1996a), periaqueductal gray (Vaughan et al., 1997), nucleus raphe magnus (Pan et al., 2000) and in cultured tuberomammillary neurons (Bajic et al., 2004). The activation of GIRK channels results in a dominant outward current (or hyperpolarization) at resting membrane potentials due to the selective efflux of  $\text{K}^+$  (Rudy, 1988). The ability of the NOP receptor to both presynaptically inhibit glutamatergic neurotransmission and postsynaptically activate GIRK1 channels would ultimately lead to a powerful inhibition of anorexigenic POMC neurons. This may well account for the NOP receptor-mediated increase in food intake and the microstructural changes in meal pattern observed in this and other studies.

This does not mean that the NOP receptor-mediated changes in food intake and meal pattern are due exclusively to alterations in the activity of POMC neurons. OFQ/N has been shown to respectively increase and decrease the gene expression of orexigenic AgRP and

anorexigenic CART in chick diencephalon (Bungo et al., 2009), which is corroborated by parallel changes in the release of these peptides in rat hypothalamic explants (Bewick et al., 2005). In addition, hyperphagic responses are elicited upon focal injection of OFQ/N into the nucleus accumbens, and the hypothalamic paraventricular nucleus, VMN and ARC (Stratford et al., 1997; Polidori et al., 2000b). Among these injected sites, however, it is the ARC that yields the most robust hyperphagic response (Polidori et al., 2000b). While the NOP receptor is clearly found in AgRP neurons, it is also expressed in CART neurons, including those in the ARC (Bewick et al., 2005). Given the extensive colocalization of CART in POMC neurons (Horvath, 2005), and the fact that we recorded from OFQ-responsive  $\alpha$ -MSH-immunopositive cells, it stands to reason that the NOP receptor is expressed in these cells as well. Thus, while OFQ/N can evoke hyperphagia from a multiplicity of sites, it is clear that the ARC is a fundamentally important neuroanatomical substrate, and that pleiotropic actions at POMC synapses make a significant contribution to the NOP receptor-mediated regulation of food intake and meal pattern. Future studies designed to test whether the OFQ-induced hyperphagia is blocked by melanocortin receptor antagonists, or diminished in POMC-deficient mice, will further confirm our working hypothesis.

In conclusion, these results reveal that NOP receptor activation stimulates food intake, regulates meal pattern and inhibits the excitability of ARC POMC neurons. These findings indicate that the NOP receptor-mediated hyperphagia involves a disinhibition of the anorexigenic control systems in the mediobasal hypothalamus, and help further define the role of the NOP receptor in energy homeostasis.

## Acknowledgements

Grant support: This study was supported by PHS Grants HD058638 (sub-contract to EJW) and DA016882 (to KL), and an intramural research grant from Western University of Health Sciences (to EJW).

## Appendix. Supplementary material

Supplementary data associated with this article can be found in the online version, at doi:10.1016/j.neuropharm.2010.05.007.

## References

- Abdulla, F.A., Smith, P.A., 1997. Nociceptin inhibits T-type  $\text{Ca}^{2+}$  channel current in rat sensory neurons by a G-protein-independent mechanism. *J. Neurosci.* 17, 8721–8728.
- Allen, C.N., Jiang, Z.-G., Teshima, K., Darland, T., Ikeda, M., Nelson, C.S., Quigley, D.I., Yoshioka, T., Allen, R.G., Rea, M.A., Grandy, D.K., 1999. Orphanin-FQ/nociceptin (OFQ/N) modulates the activity of suprachiasmatic nucleus neurons. *J. Neurosci.* 19, 2152–2160.
- Appleyard, S.M., Hayward, M., Young, J.I., Butler, A.A., Cone, R.D., Rubinstein, M., Low, M.J., 2003. A role for endogenous  $\beta$ -endorphin in energy homeostasis. *Endocrinology* 144, 1753–1760.
- Bajic, D., Hoang, Q.V., Nakajima, S., Nakajima, Y., 2004. Dissociated histaminergic neuron cultures from the tuberomammillary nucleus of rats: culture methods and ghrelin effects. *J. Neurosci. Methods* 132, 177–184.
- Bewick, G.A., Dhillon, W.S., Darch, S.J., Murphy, K.G., Gardiner, J.V., Jethwa, P.H., Kong, W.M., Ghatei, M.A., Bloom, S.R., 2005. Hypothalamic cocaine- and amphetamine-regulated transcript (CART) and agouti-related protein (AgRP) neurons coexpress the NOP1 receptor and nociceptin alters CART and AgRP release. *Endocrinology* 146, 3526–3534.
- Bianchi, C., Marani, L., Barbieri, M., Marino, S., Beani, L., Siniscalchi, A., 2004. Effects of nociceptin/orphanin FQ and endomorphin-1 on glutamate and GABA release, intracellular  $[\text{Ca}^{2+}]$  and cell excitability in primary cultures of rat cortical neurons. *Neuropharmacology* 47, 873–883.
- Blakley, G.G., Pohorecky, L.A., Benjamin, D., 2004. Behavioral and endocrine changes following antisense oligonucleotide-induced reduction in the rat NOP receptor. *Psychopharmacology (Berl.)* 171, 421–428.
- Bomberg, E.M., Grace, M.K., Levine, A.S., Olszewski, P.K., 2006. Functional interaction between nociceptin/orphanin FQ and  $\alpha$ -melanocyte-stimulating hormone in the regulation of feeding. *Peptides* 27, 1827–1834.
- Brann, D.W., Mahesh, V.B., 1995. Glutamate: a major neuroendocrine excitatory signal mediating steroid effects on gonadotropin secretion. *J. Steroid Biochem. Mol. Biol.* 53, 325–329.
- Bungo, T., Shiraishi, J., Yanagita, K., Ohta, Y., Fujita, M., 2009. Effect of nociceptin/orphanin FQ on feeding behavior and hypothalamic neuropeptide expression in layer-type chicks. *Gen. Comp. Endocrinol.* 163, 47–51.
- Bunzow, J.R., Saez, C., Mortrud, M., Bouvier, C., Williams, J.T., Low, M., Grandy, D.K., 1994. Molecular cloning and tissue distribution of a putative member of the rat opioid receptor gene family that is not a  $\mu$ ,  $\delta$  or  $\kappa$  opioid receptor type. *FEBS Lett.* 347, 284–288.
- Challis, B.G., Coll, A.P., Yeo, G.S.H., Pinnock, S.B., Dickson, S.L., Thresher, R.R., Dixon, J., Zahn, D., Rochford, J.J., White, A., Oliver, R.L., Millington, G., Aparicio, S.A., Colledge, W.H., Russ, A.P., Carlton, M.B., O'Rahilly, S., 2004. Mice lacking proopiomelanocortin are sensitive to high-fat feeding but respond normally to the acute anorectic effects of peptide-YY<sub>3–36</sub>. *Proc. Natl. Acad. Sci. U.S.A.* 101, 4695–4700.
- Chen, X., McClatchy, D.B., Geller, E.B., Liu-Chen, L.-Y., Tallarida, R.J., Adler, M.W., 2001. Possible mechanism of hypothermia induced by intracerebroventricular injection of orphanin FQ/nociceptin. *Brain Res.* 904, 252–258.
- Connor, M., Vaughan, C.W., Chieng, B., Christie, M.J., 1996a. Nociceptin receptor coupling to a potassium conductance in rat locus coeruleus neurones *in vitro*. *Br. J. Pharmacol.* 119, 1614–1618.
- Connor, M., Yeo, A., Henderson, G., 1996b. The effect of nociceptin on  $\text{Ca}^{2+}$  channel current and intracellular  $\text{Ca}^{2+}$  in the SH-SY5Y human neuroblastoma cell line. *Br. J. Pharmacol.* 118, 205–207.
- Diaz, S., Farhang, B., Hoiem, J., Stahlman, M., Adatia, N., Cox, J.M., Wagner, E.J., 2009. Sex differences in the cannabinoid modulation of appetite, body temperature and neurotransmission at POMC synapses. *Neuroendocrinology* 89, 424–440.
- Economidou, D., Policani, F., Angellotti, T., Massi, M., Terada, T., Ciccocioppo, R., 2006. Effect of novel NOP receptor ligands in food intake in rats. *Peptides* 27, 775–783.
- Emmerson, P.J., Miller, R.J., 1999. Pre- and postsynaptic actions of opioid and orphan opioid agonists in the rat arcuate nucleus and ventromedial hypothalamus *in vitro*. *J. Physiol. (Lond.)* 517, 431–445.
- Gompf, H.S., Moldavan, M.G., Irwin, R.P., Allen, C.N., 2005. Nociceptin/orphanin FQ (N/OFQ) inhibits excitatory and inhibitory synaptic signaling in the suprachiasmatic nucleus (SCN). *Neuroscience* 132, 955–965.
- Ho, J., Cox, J.M., Wagner, E.J., 2007. Cannabinoid-induced hyperphagia: correlation with inhibition of proopiomelanocortin neurons? *Physiol. Behav.* 92, 507–519.
- Horvath, T.L., 2005. The hardship of obesity: a soft-wired hypothalamus. *Nat. Neurosci.* 8, 561–565.
- Knoflach, F., Reinscheid, R.K., Civelli, O., Kemp, J.A., 1996. Modulation of voltage-gated calcium channels by orphanin FQ in freshly dissociated hippocampal neurons. *J. Neurosci.* 16, 6657–6664.
- Koizumi, M., Cagniard, B., Murphy, N.P., 2009. Endogenous nociceptin modulates diet preference independent of motivation and reward. *Physiol. Behav.* 97, 1–13.
- Lambert, P.D., Couceyro, P.R., McGirr, K.M., Dall Vechia, S.E., Smith, Y., Kuhar, M.J., 1998. CART peptides in the central control of feeding and interactions with neuropeptide Y. *Synapse* 29, 293–298.
- Matsushita, H., Ishihara, A., Mashiko, S., Tanaka, T., Kanno, T., Iwaasa, H., Ohta, H., Kanatani, A., 2009. Chronic intracerebroventricular infusion of nociceptin/orphanin FQ produces body weight gain by affecting both feeding and energy metabolism. *Endocrinology* 150, 2668–2673.
- Matthes, H., Seward, E.P., Kieffer, B., North, R.A., 1996. Functional selectivity of orphanin FQ for its receptor coexpressed with potassium channel subunits in *Xenopus laevis* oocytes. *Mol. Pharmacol.* 50, 447–450.
- Meis, S., Pape, H.-C., 2001. Control of glutamate and GABA release by nociceptin/orphanin FQ in the rat lateral amygdala. *J. Physiol. (Lond.)* 532, 701–712.
- Meunier, J.-C., Mollereau, C., Toll, L., Suaudeau, C., Moisand, C., Alvinerie, P., Butour, J.-L., Guillemot, J.-C., Ferrara, P., Monsarrat, B., Mazarguil, H., Vassart, G., Permentier, M., Constantin, J., 1995. Isolation and structure of the endogenous agonist of opioid receptor-like ORL1 receptor. *Nature* 377, 532–535.
- Mollereau, C., Parmentier, M., Mailleux, P., Butour, J.-L., Moisand, C., Chalon, P., Caput, D., Vassart, G., Meunier, J.-C., 1994. ORL1, a novel member of the opioid receptor family. *FEBS Lett.* 341, 33–38.
- Morgan, C.A., Emmans, G.C., Tolcamp, B.J., Kyriazakis, I., 2000. Analysis of the feeding behavior of pigs using different models. *Physiol. Behav.* 68, 395–403.
- Pan, Z.Z., Hirakawa, N., Fields, H.L., 2000. A cellular mechanism for the bidirectional pain-modulating actions of orphanin FQ/nociceptin. *Neuron* 26, 515–522.
- Polidori, C., Calo', G., Ciccocioppo, R., Guerini, R., Regoli, D., Massi, M., 2000a. Pharmacological characterization of the nociceptin mediating hyperphagia: identification of a selective antagonist. *Psychopharmacology (Berl.)* 148, 430–437.
- Polidori, C., de Caro, G., Massi, M., 2000b. The hyperphagic effect of nociceptin/orphanin FQ in rats. *Peptides* 21, 1051–1062.
- Pomonis, J.D., Billington, C.J., Levine, A.S., 1996. Orphanin FQ, agonist of the orphan opioid receptor, stimulates feeding in rats. *Neuroreport* 8, 369–371.
- Reinscheid, R.K., Nothacker, H.-P., Boursion, A., Ardati, A., Henningsen, R.A., Bunzow, J.R., Grandy, D.K., Langen, H., Monsma, F.J., Civelli, O., 1995. Orphanin FQ: a neuropeptide that activates an opioidlike G protein-coupled receptor. *Science* 270, 792–794.

- Ronnekleiv, O.K., Loose, M.D., Erickson, K.R., Kelly, M.J., 1990. A method for immunocytochemical identification of biocytin-labeled neurons following intracellular recording. *BioTechniques* 9, 432–438.
- Rudy, B., 1988. Diversity and ubiquity of K channels. *Neuroscience* 25, 729–749.
- Sinchak, K., Dewing, P., Cook, M., Micevych, P.E., 2007. Release of orphanin FQ/nociceptin in the medial preoptic nucleus and ventromedial nucleus of the hypothalamus facilitates lordosis. *Horm. Behav.* 51, 406–412.
- Sinchak, K., Romeo, H.E., Micevych, P.E., 2006. Site-specific estrogen and progesterone regulation of orphanin FQ/nociceptin and nociceptin opioid receptor mRNA expression in the female rat limbic hypothalamic system. *J. Comp. Neurol.* 496, 252–268.
- Stratford, T.R., Holahan, M.R., Kelley, A.E., 1997. Injections of nociceptin into the nucleus accumbens shell or ventromedial hypothalamic nucleus increase food intake. *Neuroreport* 8, 423–426.
- Tajalli, S., Jonaidi, H., Abbasnejad, M., Denbow, D.M., 2006. Interaction between nociceptin/orphanin FQ (N/OFQ) and GABA in response to feeding. *Physiol. Behav.* 89, 410–413.
- Uezu, K., Sei, H., Sano, A., Toida, K., Suzuki-Yamamoto, T., Houtani, T., Sugimoto, T., Takeshima, H., Ishimura, K., Morita, Y., 2004. Lack of nociceptin receptor alters body temperature during resting period in mice. *Neuroreport* 15, 751–755.
- van den Pol, A.N., Wuarin, J.P., Dudek, F.E., 1990. Glutamate, the dominant excitatory transmitter in neuroendocrine regulation. *Science* 250, 1276–1278.
- Vaughan, C.W., Christie, M.J., 1996. Increase by the ORL<sub>1</sub> receptor (opioid receptor-like<sub>1</sub>) ligand, nociceptin, of inwardly rectifying K conductance in dorsal raphe neurones. *Br. J. Pharmacol.* 117, 1609–1611.
- Vaughan, C.W., Ingram, S.L., Christie, M.J., 1997. Actions of the ORL<sub>1</sub> receptor ligand nociceptin on membrane properties of rat periaqueductal gray neurons *in vitro*. *J. Neurosci.* 17, 996–1003.
- Wagner, E.J., Rønnekleiv, O.K., Grandy, D.K., Kelly, M.J., 1998. The peptide orphanin FQ inhibits  $\beta$ -endorphin neurons and neurosecretory cells in the hypothalamic arcuate nucleus by activating an inwardly-rectifying K<sup>+</sup> conductance. *Neuroendocrinology* 67, 73–82.
- Zhang, S., Yu, L., 1995. Identification of dynorphins as endogenous ligands for an opioid receptor-like orphan receptor. *J. Biol. Chem.* 270, 22772–22776.